

Controlled deposition of nanotubes on opposing electrodes

Shaoning Lu, Jaehyun Chung and Rodney S Ruoff¹

Department of Mechanical Engineering, Northwestern University, 2145 Sheridan Road, Evanston, IL 60208-3111, USA

E-mail: r-ruoff@northwestern.edu

Received 19 January 2005, in final form 2 June 2005

Published 18 July 2005

Online at stacks.iop.org/Nano/16/1765

Abstract

We report a method of depositing individual ‘templated carbon nanotubes’ (T-CNTs) on opposing electrodes so that they are suspended across 100 μm deep trenches, and in separate experiments across low profile (70 nm thick) opposing electrodes. The geometry of the electrodes with deep trenches was chosen to be essentially identical to that in a micro-electromechanical system (MEMS) testing stage used for mechanical loading of nanostructures. An electric field was used to attract the T-CNTs dispersed in a solvent and critical point drying was employed to protect them from breaking or deforming. The real-time potential change in the circuit was monitored as a means of characterizing the deposition of an individual T-CNT across this deep trench. For the case of sequential deposition on electrodes that are 70 nm above the substrate surface, a method was developed for counting the number of sequentially deposited T-CNTs. Simultaneous video recording of the deposition of T-CNTs confirmed the measured real-time potential changes for both cases. It was found that the resistance of the circuit changed as each new T-CNT was deposited for the sequential deposition; up to five T-CNTs were sequentially detected. This approach allows for controlled deposition of one-dimensional nanostructures for their potential use in NEMS devices, and may be useful for large-scale integration.

1. Introduction

The integration of suspended one-dimensional nanostructures into MEMS devices is essential for building hybrid nanoelectromechanical systems (NEMS) that exploit nanostructures’ electrical and mechanical properties. For example, single-walled carbon nanotubes (SWCNTs) have been suspended and locally probed with an AFM tip [1, 2]. We recently reported a novel MEMS testing stage with $\sim 130 \mu\text{m}$ deep trenches having nanoscale displacement for direct tensile testing experiments [3]. One challenge in using such testing stages is to successfully deposit the individual nanostructure specimens where desired.

There are already many reports on the fabrication of suspended CNTs. Deposition from CNT dispersions in liquid and direct growth by chemical vapour deposition (CVD) are two methods that have been used for suspending CNTs [4–7].

With the exception of the growth from patterned catalyst particles [6], these methods are not designed for selective deposition. CNTs are present essentially randomly on the surface and suitable candidates are found by SEM imaging; electrodes are then patterned by the relatively slow process of e-beam lithography. Thermal CVD growth of SWCNTs from patterned catalyst particles was found to be dependent on the electrode being Mo. Other metals, including gold (Au), titanium (Ti), tantalum (Ta), and tungsten (W), all failed for various reasons, including the chemicals and high temperatures used in the CVD growth [6].

Electric-field-assisted deposition has recently been used for CNTs and nanowires [8–11]. However, no deposition of CNTs or nanowires over deep trenches or free-standing MEMS devices has been reported. There are additional factors present for deposition onto three-dimensional structures with deep trenches, related to fluid dynamics and electrokinetic effects. In addition, identification of when a nanostructure has spanned both electrodes is relevant for knowing if an electrode pair

¹ Author to whom any correspondence should be addressed.

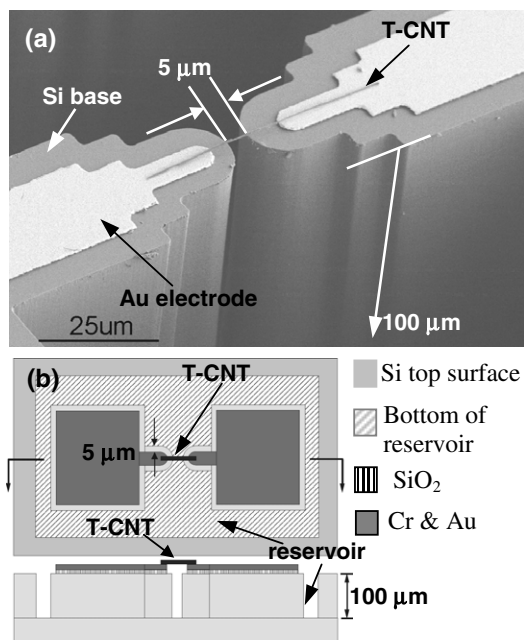


Figure 1. (a) SEM image of a T-CNT deposited across opposing electrodes separated by a 5 μm wide, 100 μm deep gap; (b) schematic top view and side view of the structure in (a).

is indeed ‘wired up’ and also for monitoring sequential depositions (should they occur) of more nanostructures. The detection of a voltage change upon deposition of a bundle of SWCNTs across electrodes with no deep trench has been reported [8], but there has been no report of the detection of each sequential deposition when multiple nanostructures are deposited.

We report here on suspending individual templated CNTs (T-CNTs) over high-aspect-ratio micromachined trenches of 100 μm deep. This was achieved with electric field guided deposition, critical point drying (CPD; Polaron E3000), and a reservoir enclosing the electrode pair. The reservoir and CPD eliminate breakage or deformation of the T-CNTs. Figure 1 shows a typical result, with a $\sim 50 \mu\text{m}$ long T-CNT suspended on a pair of electrodes. The electrodes are 100 μm above the trench bottom surface. We also observed that the number of T-CNTs being deposited is controllable by detecting voltage signal changes in the circuit. We confirmed this by video recording the deposition while measuring the circuit.

2. Experiment and discussions

The T-CNTs were grown by the porous alumina template method [12, 13], and were dispersed in 100% ethanol by sonication (175HT Tru-SweepTM) for ~ 5 min prior to each deposition run. The average T-CNT length was ~ 50 – $60 \mu\text{m}$, and the diameters ranged from 250 to 350 nm. The 3D gap structure was made with microfabrication. In figure 1(b), Cr (10 nm) and Au (100 nm) were first deposited (SC4500, CVC) on a Si wafer with 500 nm thick thermal oxide. The metals were then patterned as electrodes, and the underlying oxide was etched with the same shape by buffered oxide etching to provide electrical isolation. The deep

Si structure, which extends 5 μm beyond the edges of the metal electrodes, was obtained by using deep reactive ion etching (DRIE, Unaxis 770). A 5 μm wide, 100 μm deep, 20:1 aspect ratio gap was thereby obtained between the two high-aspect-ratio ‘Si bases’ (figure 1(a)). A reservoir was designed and fabricated to enclose all these microstructures (figure 1(b)). With this reservoir, a volume of liquid (ethanol in this case) can be held so that the liquid does not spread and evaporate too quickly before the chip is transferred to the CPD apparatus.

A composite electrical field with ac (5 MHz) and dc components was applied between the Au electrodes with a pair of tungsten probes connected to power supplies (Agilent 33120A function generator (ac) and Agilent 6544A dc power supply). The experiments were conducted on a probe station (Wentworth MP0950) equipped with an optical microscope (Bausch & Lomb MicroZoomTM) for observation. A CCD camera (Hitachi HV-C20M) was connected to the microscope for video recording with a speed of 30 frames s^{-1} . To deposit T-CNTs over the 100 μm deep trench, approximately 20 μl of T-CNT/ethanol dispersion was dropped onto the chip with a pipette (Eppendorf Research). It was observed (and video recorded) that the T-CNTs aligned with the applied electric field and that they were directed to the gap region.

After one or several T-CNTs were deposited across the gap, the power was manually turned off. Prior to the ethanol droplet completely drying out, the sample was completely submerged into a 20 ml beaker filled with ~ 15 ml of 100% ethanol, and taken to the CPD, where the sample was transferred into the CPD boat filled with ethanol. The ethanol was then substituted with liquid CO_2 and the sample was run through the critical point drying process. Without the CPD, the surface tension from the drying liquid (meniscus-driven assembly) tends to drive the T-CNTs into a bundle (when multiple T-CNTs are present from the prior deposition process), and an out-of-plane force (component of the capillary force) also acts to draw the T-CNTs to the bottom of the trenches or to bend them, as observed with the light microscope. With the aid of CPD and the reservoir, it was possible to minimize these forces and to suspend the T-CNTs without any bending or bundling. The adhesion between the T-CNTs and the Au electrodes was strong enough to survive the transfer and drying process. We note that this process is currently being used for depositing T-CNTs onto MEMS testing stages similar to those reported [3] but with 100 μm deep trenches between opposing platforms. To perform tensile loading experiments on these and other nanostructures it is necessary to clamp the structures at each platform (electrode). A typical method used by our group and others is to deposit clamps by the electron beam induced decomposition method (EBID). The EBID method has been demonstrated to be a reasonably effective method for clamping nanostructures for mechanical testing [14, 15].

Experiments were conducted to see if there was a correlation between the video recording of T-CNT depositions and the change in electric potential as a function of time between the electrodes. The upper inset of figure 2 shows the circuit used for depositions across electrodes with the same type of deep trench as in figure 1. The dc potential between electrodes (V_{dc}) was monitored while the deposition(s) were video recorded. The voltage signals were first amplified by

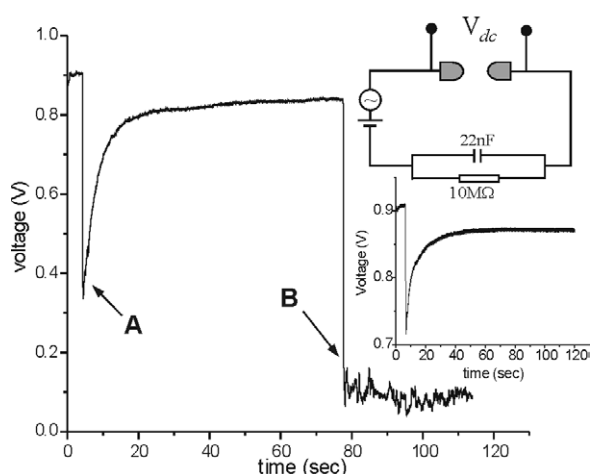


Figure 2. Voltage as a function of time across opposing electrodes with the same structure as shown in figure 1, during the process of T-CNT deposition. The upper inset shows the circuit used. The source signal is 8 V_{p-p} (ac), 1 V (dc), and $f = 5$ MHz. The lower inset shows the voltage change when pure ethanol is dropped onto this device.

a low noise preamplifier (Stanford Research Systems SR560; input resistance 100 M Ω) having a built-in 30 Hz low pass filter, so as to remove the 5 MHz component. Next, the signals were run through a second low pass filter of 10 Hz (Krohn-Hite 3945), and the final V_{dc} signals were collected by a data acquisition system (National Instrument DAQ 6036E) with a sampling rate of 100 Hz. When a composite field of ac with dc offset is applied over the gap through the capacitor and resistor, the T-CNTs are attracted and aligned; a composite field has also been used for deposition of MWCNTs across electrode pairs but without a deep trench [10]. When a T-CNT electrically bridges the gap, a dc current passes through the 10 M Ω reference resistor. The value of the reference resistor determines the sensitivity of the system, in terms of the number of T-CNTs that can be attracted and detected. For example, the initial resistance across the gap is ~ 150 M Ω when the T-CNT/ethanol dispersion is added, and the resistance of a T-CNT deposited across the electrodes is ~ 10 M Ω (including its contact resistance in the presence of ethanol). The 10 M Ω reference resistor (not to be confused with the ~ 10 M Ω contact resistance of the T-CNT) would thus decrease the dc potential across the gap by 44% when a T-CNT is deposited. Increasing the reference resistance, for example to 50 M Ω , would decrease the $V_{dc} \sim 58\%$. In other words, the larger the reference resistance, the smaller the number of T-CNTs that can be readily detected after the first T-CNT is deposited. In addition, if the reference resistance is increased the initial electrical field across the gap will be weakened and the attraction of the first T-CNT would be decreased. The attraction of other T-CNTs into the region of the opposing electrodes is a function of the magnitude of the electric field, which is smaller (with a larger reference resistance) after the first T-CNT is deposited. A similar method was, e.g., used (with a 1 G Ω resistor) to prevent multiple deposition of Pd particles [16].

Figure 2 shows a plot of V_{dc} (between the electrodes) versus time for the case of a single T-CNT bridging a gap

of the same dimensions as shown in figure 1. The initial V_{dc} is that of a dry sample in air, indicated by the value of ~ 0.9 V. At the moment when a drop of T-CNT/ethanol dispersion was placed onto the chip, the V_{dc} dropped to point 'A'. This drop was followed by an increase for ~ 36 s until the potential reached a nearly constant value. As video recorded, at 73.23 ± 0.03 s after the droplet was deposited, a T-CNT was deposited such that both its ends were in contact with the opposing Au electrodes. This generated a second sharp V_{dc} drop 'B' in figure 2, which also started 73.37 ± 0.01 s after the droplet was deposited. The digitized frame-grabbed image showing the T-CNT contacting both electrodes thus coincides in time with the electrically recorded signature of this event.

The process of electrically recording when deposition occurred can also be presented in terms of resistance between the electrodes (by converting the voltage into resistance). The calibration was done by replacing the sample with standard resistors and measuring the voltage across them. When the T-CNT/ethanol dispersion was placed on the electrodes, the resistance decreased from infinite to a few mega ohms and then increased back to ~ 150 M Ω . In order to confirm that the second voltage drop was caused by the deposited T-CNT, a similar volume of pure ethanol (without T-CNTs) was dropped onto the same device with identical input signals. The lower inset of figure 2 shows the measured V_{dc} versus time. The first voltage drop was again observed but not the second. We speculate that the ethanol is electrolysed under the electric field strength employed ($E_{dc} = 0.07$ V μm^{-1} , $E_{ac(rms)} = 0.19$ V μm^{-1}), and that this results in the sudden drop of resistance at the beginning. The recovery time τ (the time to reach a nearly constant value of the potential), after the initial voltage drop was 36 seconds and can be explained by an electrical double layer forming near the electrodes. The capacitance attributed to the double layer was measured by linear potential sweep voltammetry (CH Instruments Electrochemical Analyzer model 710B) for the deep trench structure. The capacitance (C) attributed to the presence of a double layer was found to be 240 nF. The calculated time constant ($\tau = C \cdot R$) is 36 s, where $R = 150$ M Ω (the measured resistance of ethanol between these two electrodes). This value of 36 s is identical with the experimentally measured rise time for ethanol and T-CNT/ethanol dispersion. The appearance of a T-CNT across the electrodes changes the electric field and ion distribution.

The real-time detection of sequential deposition of individual T-CNTs was achieved using a reference resistor of 15 k Ω . For the study of sequential deposition, 70 nm thick electrodes (10 nm Cr/60 nm Au) on top of Si (itself coated with a 500 nm thick SiO₂ layer) were used, as shown in figure 3(a). Figures 3(b)–(f) are individual digitized frames from the video recording of sequential deposition of five T-CNTs. In this case, the dc potential (V_{dc}) was measured (with the same preamplifier, filter and DAQ as above) across the 15 k Ω reference resistor in order to decrease the effect of the input resistance (100 M Ω) from the preamplifier. The circuit is shown in figure 4. The measured V_{dc} increased as T-CNTs were deposited over the gap. In figure 4, the first increase in V_{dc} occurred when T-CNT/ethanol dispersion was applied ('A') at 5.24 ± 0.01 s. At 16.51 ± 0.01 s, the first T-CNT ('1') was spanning the electrodes. The second T-CNT deposited

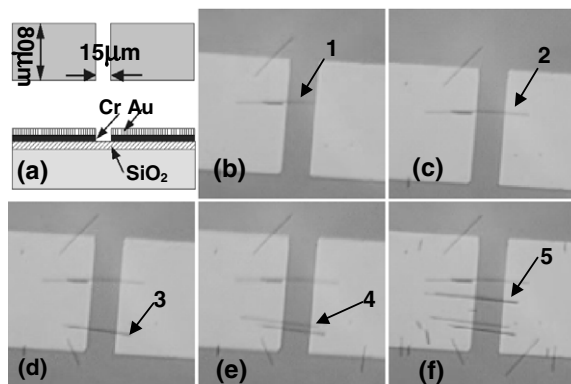


Figure 3. (a) Schematic diagram of the device design having opposing electrodes that project 70 nm from the SiO₂/Si surface; (b)–(f) frame-grabbed digitized video images of T-CNTs that were deposited in sequence across electrodes separated by a 15 μm gap; the initial time of $t = 0$ (for the images) was chosen to be when the T-CNT/ethanol droplet was applied; (b) $t = 11.33 \pm 0.03$ s; (c) $t = 19.46 \pm 0.03$ s; (d) $t = 21.50 \pm 0.03$ s; (e) $t = 28.90 \pm 0.03$ s; (f) $t = 53.63 \pm 0.03$ s.

such that it overlapped the first one (figure 3(c)), resulting in a further decrease in the gap voltage and an increase in the voltage across the 15 kΩ resistor at 24.67 ± 0.01 s (figure 4). V_{dc} also increased at 26.68 ± 0.01 s, 34.07 ± 0.01 s and 58.84 ± 0.01 s (figure 4), which coincided with the video recorded time for the third, fourth, and fifth T-CNTs deposited, as shown in figures 3(d)–(f). Although the ethanol evaporates more rapidly over this 70 nm (shallow) trench, the ethanol was present as each of these T-CNTs were deposited across the opposing electrodes. The T-CNTs deposited across the electrodes maintained the same position after drying. Figure 5 shows such an example (on a different pair of electrodes). The video recorded image at the end of a deposition experiment before the ethanol dried out is shown in figure 5(a), and figure 5(b) is an SEM image of the same region after drying. The position and orientation of the T-CNTs in these two images are essentially identical. Thus, it should be possible to control the number of T-CNTs to be deposited by monitoring the changes in circuit response with time (and by using feedback).

Experiments were undertaken to detect the sequential deposition of more than one T-CNT across the 100 μm deep trench structure. It was possible (six separate experiments in total) to recognize the deposition of the first T-CNT (with the 10 MΩ reference resistor); the video record agreed with the time signature of the voltage change. However, it was not possible to reliably detect the deposition of a second T-CNT (five of the six experiments), nor of a third T-CNT (one experiment), with the 10 MΩ reference resistor. Neither the first nor subsequently deposited T-CNTs could be reliably identified from the voltage versus time data alone, when a 15 kΩ reference resistor was used (ten separate experiments). Thus, there is a difference in our current ability to determine reliably the sequential deposition of T-CNTs across the deep trench structure, as opposed to the low profile (70 nm thick electrodes) structure described above.

The resistance between the two metal electrodes in the deep trench structure when immersed in pure ethanol is ~ 150 MΩ at equilibrium; with no ethanol present the circuit

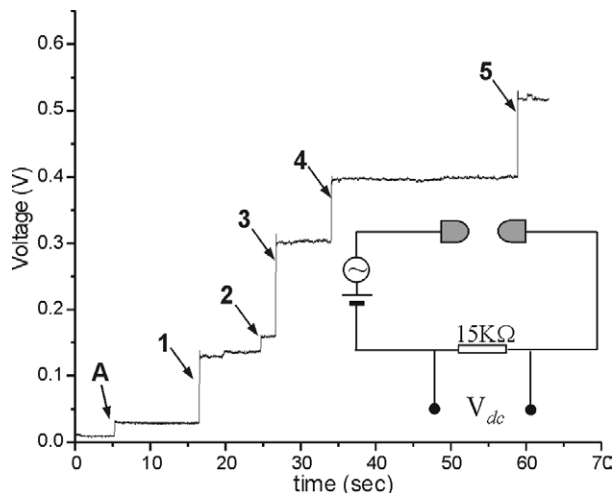


Figure 4. The series of five voltage changes across the 15 kΩ reference resistor, corresponding to the five T-CNTs sequentially deposited in figure 3. The source signal is 20 V_{p-p} (ac), 1.5 V (dc), and $f = 5$ MHz. The inset is the circuit diagram for this deposition experiment.

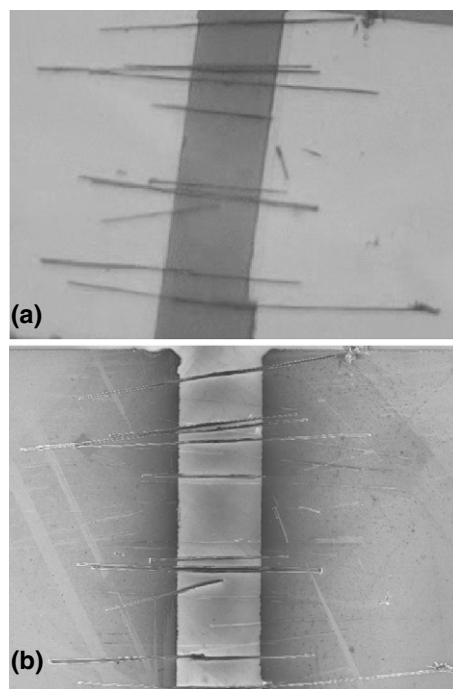


Figure 5. (a) Video recorded image (with ethanol still present) of T-CNTs deposited across ‘low-profile’ electrodes; (b) SEM image of the same electrode pair after drying of the ethanol.

is open (‘infinite’ resistance). The ~ 150 MΩ resistance with the pure ethanol is evidently due to the intrinsic resistance of ethanol. The DRIE etching typically deposits a thin fluoropolymer coating on an etched Si surface [17]; it is however possible that this is to some degree removed by other processing steps such as the Piranha etch that was used for cleaning the photoresist mask.

The deep trenches versus low profile electrodes (no trench) were evaluated in an attempt to try to understand why detection

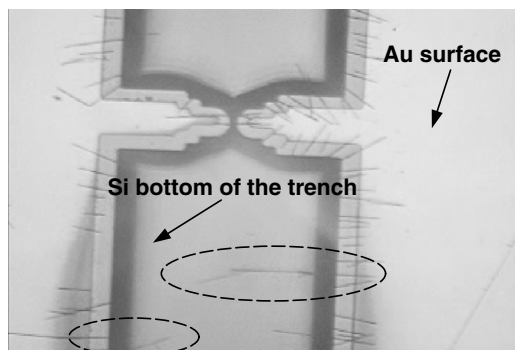


Figure 6. Examples (circled regions) of T-CNTs projecting out from the Au patterned regions and (perhaps) touching the bottom of the 100 μm deep trench during deposition.

of sequential deposition of additional T-CNTs did not work well with the deep trenches. It is possible that particles (such as T-CNTs or impurities) are deposited between the Si substrate and the Au layers (which are on top of the SiO_2 layer) on each side of the trench. It is also possible that intermittent changes in impedance of the circuit result from, e.g., T-CNTs that are projecting off from either of the Au platforms on either side of the trench. An example in figure 6 (circled regions) shows a few T-CNTs that might be either touching or close to the Si substrate at the bottom of the trench; in the presence of ethanol and given the possibility that these do not make a strong (adhesive) contact (e.g., at their tips) with the Si at the bottom of the trench, it is possible that such deposits are responsible for the sort of intermittent fluctuations observed at times during the experiments on the deep trench samples. It is our observation that such T-CNTs only stay connected with the electrical field present. Once the electrical field is removed, they (certainly a very large percentage of them) flow away in the liquid when transferred to the CPD. For the case of the low profile electrodes, the metal electrodes were fabricated on a 500 nm thick SiO_2 layer, so that the surface between the electrodes was insulated. The T-CNTs attracted to the edges of the electrodes do not contribute to the resistance change due to this insulating layer. The bottom substrate may have to be more thoroughly insulated than the 1–2 nm ‘ambient’ oxide that is present on the devices we fabricated. Experiments, e.g., on electrodes fabricated on an insulating material such as SiO_2 could test this hypothesis.

For some applications, an array of controllably deposited nanowires or nanotubes is desirable. Consider the case of 32 electrode pairs and use of a 32-channel data acquisition (DAQ) system and an appropriate control circuit for each electrode pair. It should be possible to exploit the ability to monitor the time sequence of deposition events for electrode pairs with the low profile electrode configuration (see figure 4). The mean voltage rise time in four separate experiments of sequential deposition, on the low-profile opposing electrodes, was 0.1 s (the shortest was 0.08 s; the longest was 0.17 s). The mean rise time recorded for the six separate experiments on T-CNT deposition on the deep trench structures was 0.2 s (low 0.08 s, high 0.3 s). Once a CNT is deposited across one electrode pair, the circuit for that pair can be shut down immediately. The approximate time to manually switch off the applied voltage

across the opposing electrodes is ~ 0.2 ms for the ac and dc power supplies we used, which is much shorter, for our experimental runs, than the time needed for another T-CNT to be attracted and deposited. By optimizing the concentration of T-CNTs used in the liquid dispersion, controlled assembly over even a very large array should be achievable. Active control would involve applying voltages to n electrode pairs, each pair with an appropriate control circuit (in the example above, n is 32). The number of sequentially deposited T-CNTs can be controlled for each electrode pair. As shown, we could readily detect up to five T-CNTs deposited for the low profile electrode pair. After T-CNTs are deposited across the first set of n electrode pairs, the next set of n electrode pairs could be controlled by the n -channel DAQ card, and so on (multiplexing methods could be exploited as well).

Per the discussion above, it should also be possible to deposit one and only one T-CNT on the deep trench structures. We suggest that this process might be further optimized, as our method of detection presented here was to monitor only the dc voltage. Monitoring changes in the capacitance of the circuit through changes in the ac voltage may allow for a finer level of control, and may be more useful for monitoring deposition across deep trench structures of the type discussed here.

3. Conclusions

In summary, we report a direct assembly method to suspend individual templated carbon nanotubes (T-CNTs) across opposing electrodes separated by a 100 μm trench, and of controllable sequential deposition of up to five T-CNTs across electrodes projecting 70 nm from the surface (thus not separated by a deep trench). This method allows for the positioning of nanowires between opposing electrodes at desired locations with minimal chemical or mechanical damage. By monitoring the change of electrical potential, the deposition of individual T-CNTs (during deposition of a sequence of T-CNTs) could be readily tracked from the changes in the circuit electrical response. This was proven by simultaneous video recording. Further work is necessary to see if the same level of recognition of individual deposition events can be achieved for deep trench configurations.

This technique may prove useful for large scale assembly of NEMS that have suspended nanotubes or nanowires, for developing new sensor arrays, and for deposition of nanostructures on to testing stages.

Acknowledgments

We gratefully acknowledge T Xu for supplying the T-CNTs, E Zimney for assistance with LabView software, and D R Cantrell for comments. We appreciate the support from the Naval Research Laboratory (grant No N00173-04-2-C003), the Office of Naval Research (grant No N000140210870) and the NSF (CMS-0304506; NIRT: ‘Synthesis, characterization and modeling of aligned nanotube arrays for nanoscale devices’, programme manager Ken Chong). The fabrication work was performed in part at the Cornell Nano-Scale Science and Technology Facility (a member of the National Nanofabrication Users Network), which is supported by the

National Science Foundation under grant ECS-9731293, its users, Cornell University and industry affiliates.

References

- [1] Walters D A, Ericson L M, Casavant M J, Liu J, Colbert D T, Smith K A and Smalley R E 1999 *Appl. Phys. Lett.* **74** 3803
- [2] Tomblor T W, Zhou C, Alexseyev L, Kong J, Dai H, Liu L, Jayanthi C S, Tang M and Wu S-Y 2000 *Nature* **405** 769
- [3] Lu S, Dikin D D, Zhang S, Fisher F T, Lee J and Ruoff R S 2004 *Rev. Sci. Instrum.* **75** 2154
- [4] Babic B, Furer J, Sahoo S, Farhangfar S and Schönenberger C 2003 *Nano Lett.* **3** 1577
- [5] Lee S-B, Teo K B K, Amaratunga G A J, Milne W I, Chhowalla M, Hasko D G and Ahmed H 2003 *J. Vac. Sci. Technol. B* **21** 996
- [6] Franklin N R, Wang Q, Tomblor T W, Javey A, Shim M and Dai H 2002 *Appl. Phys. Lett.* **81** 913
- [7] Nygard J and Cobden D H 2001 *Appl. Phys. Lett.* **79** 4216
- [8] Krupke R, Hennrich F, Weber H B, Beckmann D, Hampe O, Malik S, Kappes M M and Löhneysen H V 2003 *Appl. Phys. A* **76** 397
- [9] Krupke R, Hennrich F, Weber H B, Kappes M M and Löhneysen H V 2003 *Nano Lett.* **3** 1019
- [10] Chung J, Lee K-H, Lee J and Ruoff R S 2004 *Langmuir* **20** 3011
- [11] Smith P A, Nordquist C D, Jackson T N, Mayer T S, Martin B R, Mbindyo J and Mallouk T E 2000 *Appl. Phys. Lett.* **77** 1399
- [12] Xu T T, Piner R D and Ruoff R S 2003 *Langmuir* **19** 1443
- [13] Xu T T, Fisher F T, Brinson L C and Ruoff R S 2003 *Nano Lett.* **3** 1135
- [14] Yu M F, Lourie O, Dyer M J, Moloni K, Kelly T F and Ruoff R S 2000 *Science* **287** 637
- [15] Dong L, Arai F and Fukuda T 2002 *Appl. Phys. Lett.* **81** 1919
- [16] Bezryadin A and Dekker C 1997 *Appl. Phys. Lett.* **71** 1273
- [17] McAuley S A, Ashraf H, Atabo L, Chambers A, Hall S, Hopkins J and Nicholls G 2001 *J. Phys. D: Appl. Phys.* **34** 2679